Overview of CFD Round Robin Benchmark of the High Fidelity Fuel Rod Bundle NESTOR Experimental Data

D. M. Wells
Electric Power Research Institute
1300 West W. T. Harris Blvd., Charlotte, NC 28262, USA
dwells@epri.com

P. Peturaud
Independent Consultant
18, rue Danton, Rueil Malmaison, 92500, France
pierre.peturaud@hotmail.fr

S. K. Yagnik
Electric Power Research Institute
3420 Hillview Ave., Palo Alto, CA 94304, USA
syagnik@epri.com

ABSTRACT

Computational fluid dynamics (CFD) is becoming a vital tool to analyze the complex fluid flow and heat transfer phenomena in pressurized water reactor (PWR) cores, and its use has been increasing although only limited information is currently provided to the industry as to how the CFD analysis should be applied. In addition significant discrepancies have been observed between the CFD predictions and experimental data from rod bundle tests. This is largely due to the fact that most CFD codes have not been benchmarked against high-fidelity rod bundle data nor optimized for fuel assembly analyses.

To address such industry concerns related to the benchmarking of CFD analysis and *Best Practices* for applying CFD to PWR cores, EPRI convened a CFD round robin (RR) Group in 2009. This group included participants from fuel suppliers, CFD software developers, universities, research organizations, and utilities. The RR Participants volunteered to apply their process to the evaluation of the data from the *NESTOR* (New Experimental Studies of Thermal-Hydraulics of Rod Bundles) program collected on two 5x5 rod bundle configurations[1]. In addition to evaluating the current status of applying CFD analysis to a PWR fuel bundle, the ultimate goal of this project is development of a *Best Practices* document for CFD analyses to ultimately streamline fuel risk assessment as defined in the *Fuel Reliability Guideline: PWR Fuel Cladding Corrosion and Crud*.[2]

This paper describes the dataset from the *NESTOR* experimental program that was used in the EPRI RR activities, outlines the efforts of the EPRI CFD RR Group, and highlights the significant observations. Many of the RR Participants have related papers on their volunteered CFD analyses in this special session of NURETH-16.

KEYWORDS: fuel bundle, CFD, single-phase flow

---

[1] P. Péturaud, "Analyses of Single-Phase Heat Transfer and Onset of Nucleate Boiling in a Rod Bundle with Mixing Vane Grids", *Proceedings of the 14th International Topical Meeting on Nuclear Reactor Thermal Hydraulics (NURETH-14)*, Toronto, Ontario, Canada, September 25-30, 2011.

[2] "Fuel Reliability Guideline: PWR Fuel Cladding Corrosion and Crud, Revision 1, Volume 1, Guidance." EPRI, Palo Alto, CA: 2014. 3002002795.

1. INTRODUCTION

The EPRI Fuel Reliability Program has provided guidance to the nuclear power industry through the *Fuel Reliability Guideline: PWR Fuel Cladding Corrosion and Crud, Rev. 1* [1] to evaluate all core designs for risk associated with crud-induced power shifts (CIPS, previously axial offset anomaly, AOA) and crud-induced localized corrosion (CILC). The two phenomena are associated with the formation of corrosion product deposits (crud) on fuel cladding surfaces, which is predominately dependent of locations of sub-cooled nucleate boiling (SNB) in the core of a PWR. Depending on plant parameters, especially as they change from prior cycles with known crudding experience, to the cycle being designed, the evaluation can require the use of one of four levels of analysis to understand risk for fuel failures and/or CIPS from crud formation. Several of the defined assessment triggers, including changing system operating conditions, fuel design, core management, and chemistry or system component replacement, can require a utility to need heat transfer characteristics at discrete axial and radial locations that is only available from computational fluid dynamics (CFD) analysis.

CFD is becoming a vital tool to understand the complex fluid flow and heat transfer phenomena in pressurized water reactor (PWR) cores, and its use has been increasing in recent years. Such applications have generally proven to be useful - mainly from a qualitative point of view - but often a significant discrepancy has been observed between the CFD predictions and experimental data from rod bundle tests [2]. This is largely due to the fact that most CFD codes and application methods have not been benchmarked against high-fidelity rod bundle data nor optimized for fuel assembly analyses.

To address industry concerns related to the application of CFD to PWR cores, EPRI convened a CFD RR Group in 2009. This group included participation from fuel suppliers, CFD software developers, universities, research organizations, and utilities. The RR Participants volunteered to model a selection of experimental runs from the *NESTOR* (New Experimental Studies of Thermal-Hydraulics of Rod Bundles) program [3-6]. Ultimately, the results of the RR analysis are being leveraged to develop a CFD *Best Practices* document for CFD experts as well as for utilities interested in having single-phase flow CFD analyses performed by others to meet the requirements of the *Fuel Reliability Guideline: PWR Fuel Cladding Corrosion and Crud, Rev. 1* [1].

2. NESTOR DATASET

2.1. General

Carried out in a CEA-EDF-EPRI collaborative framework, the *NESTOR* program involved an extensive testing on identical 5×5 full length rod bundles mimicking a PWR fuel sub-assembly geometry that included (i) hydraulic isothermal experiments in the EDF-Chatou MANIVEL facility, and (ii) heated experiments in the CEA-Grenoble OMEGA facility. Two rod bundle configurations were tested in each facility:

(i) *SSG bundle configuration*: A bundle configuration, approximating 'bare' rod bundles, with grids of small size (0.8 mm high and 0.2 mm thick). This rod bundle configuration had only these simple support grids (SSG) of a dedicated CEA design (see Fig. Figure **1**(a));

(ii) *MVG bundle configuration*: An industrial bundle configuration with alternating mixing vane grids (MVG) of the Westinghouse F17x17 V5H design (see Figure 1(b)) and the SSGs, described above. From one elevation to the next one downstream, the MVGs were rotated by +90° and -90° in turn.

Figure 1(c) shows a schematic axial and cross-sectional view of the NESTOR test sections. It indicates that, with respect to most industrial PWR fuel assembly geometry, (i) the local scale in the transverse direction was 1:1, whereas (ii) the grid span length scale was roughly 1:2. Indeed, mid-span intermediate spacers (actually CEA-designed SSGs) were implemented to reasonably minimize rod bow due to magnetic forces caused by electrical current in the OMEGA bundle heater rods. Fig. 1(c) also highlights the uppermost grid spans over the 1.2 m downstream bundle length, over which axial velocity and rod wall surface temperature distributions were measured in MANIVEL and OMEGA facilities, respectively, as further discussed below.

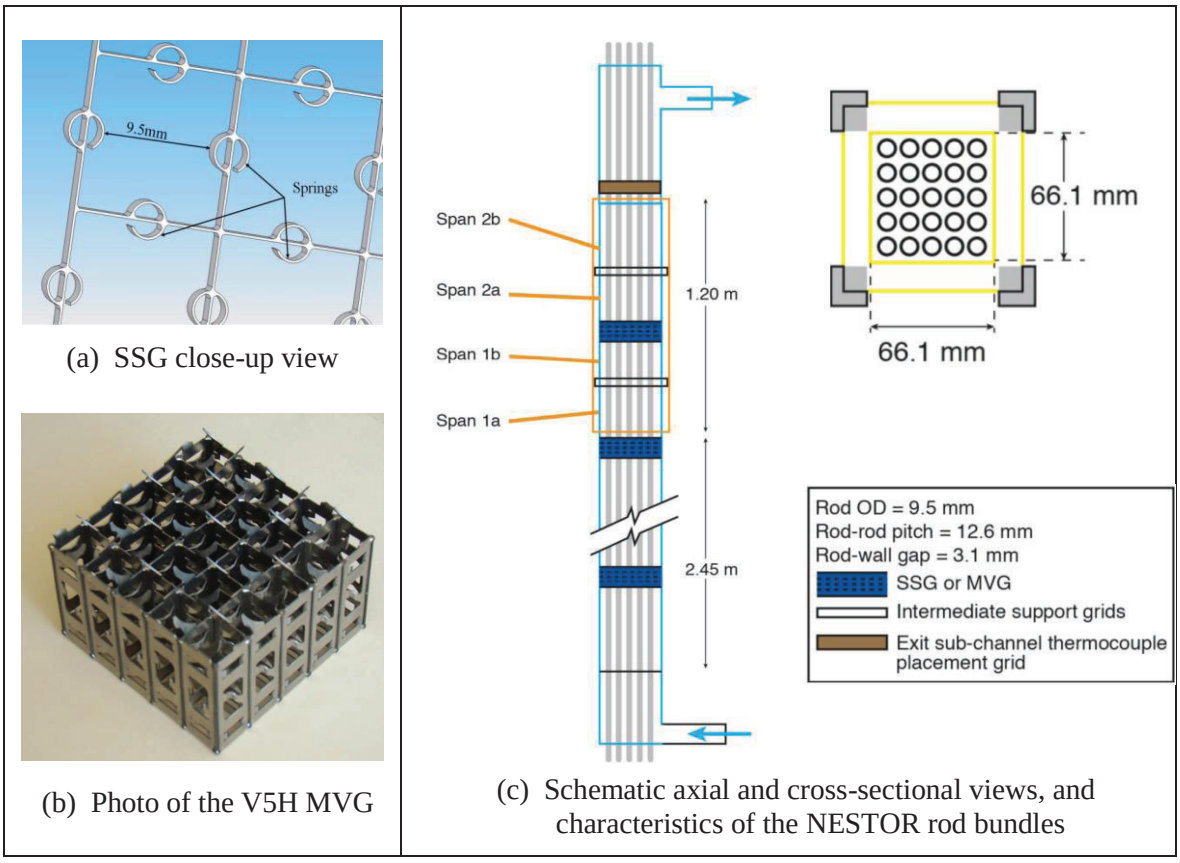

(a) SSG close-up view

(b) Photo of the V5H MVG

(c) Schematic axial and cross-sectional views, and characteristics of the NESTOR rod bundles

Figure 1. NESTOR Rod Bundle Description.

2.2. NESTOR-MANIVEL Hydraulic Isothermal Experiments

NESTOR-MANIVEL hydraulic isothermal experiments were performed in single-phase water flow at low temperature and pressure conditions and consisted of measuring (i) pressure drop, and (ii) axial velocity. Both test run types of measurements were made at steady-state volumetric flow rate and inlet temperature boundary conditions. The associated 2σ measurement uncertainties for these boundary conditions were ± 0.5% and ± 0.5 K, respectively (σ represents the standard deviation).

2.2.1. Pressure Drop Test Series

The pressure drop test series included different test runs (with several repeat runs) varying the "temperature - flow rate" condition set. The resulting Reynolds number Re_{SC}, based on the typical sub-channel hydraulic diameter and the test section averaged axial velocity, ranged from 25,000 to 140,000.

Variations in the boundary conditions during the data acquisition duration were low for each test run, with an associated variation in Re_{SC} less than 3%.

During each pressure drop test run, eight pressure taps distributed along the test section on two perpendicular walls of the casing at 279 mm axial intervals allowed redundant pressure drop measurements along a bare section of the bundle and/or across the grids (see Figure 2). The (maximum) 2σ uncertainty for these pressure drop measurements was ± 0.3 mbar.

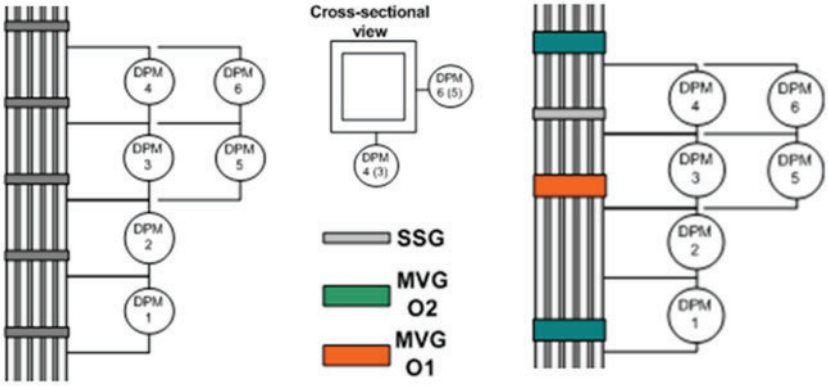

Figure 2. Pressure drop measurements along the SSG (left) and MVG (right) bundles.

Consistency checks performed on the pressure drop measurement data indicated (i) a very good repeatability with differences mostly lower than 0.5% between repeat tests, and (ii) fairly low differences (within 2% and 5% for pressure drop across MVG and SSG, respectively) between redundant measurements.

2.2.2. Axial Velocity Test Series

Detailed two-dimensional (2-D) distributions of axial velocity (both mean and root mean square fluctuations values) were obtained by means of Laser Doppler Velocimetry (LDV) scans over the bundle cross-section at several successive axial elevations in the measurement region. The related steady-state test runs had very similar volumetric flow rate, outlet temperature, and outlet pressure boundary conditions, resulting in Re_{SC} value ~ 100,000. Each set of measurements lasted up to 8 hours, but throughout the test series, variations in temperature and flow rate were low, with an associated variation in Re_{SC} less than 6% and 4% for the SSG and MVG bundle configuration tests, respectively.

The reference LDV target measurement mesh in each cross-section is given in Figure 3 and was composed of 1908 locations. Each cross-section scan was performed in two sets of 954 points each, respectively obtained along the *x* and *y* transverse directions, so that in practice, nine points were measured twice at every sub-channel center region.

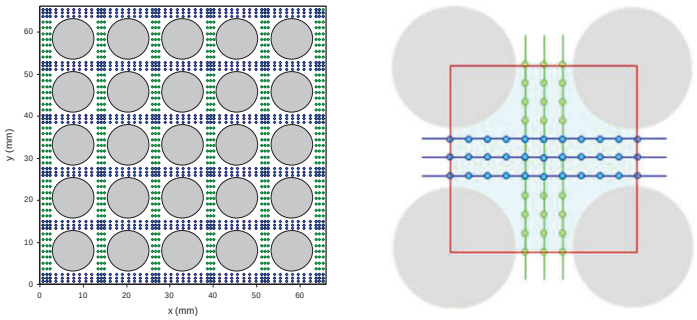

Figure 3. LDV target measurement mesh with a zoom over a typical sub-channel.

The LDV ellipsoidal measurement volume was 0.6 mm long, 0.07 mm wide and 0.07 mm high. Accurate locations were achieved by a refined geometric calibration of the LDV probe positioning system with respect to the bundle casing. As a result, the maximum positioning error was 0.2 mm in transverse *x* and *y* directions, and less than 0.5 mm in axial direction *z*.

Special attention was given to the validation of each local axial velocity measurement, accounting for specified requirements related to (i) the minimum number of validated Doppler bursts, and (ii) the maximum acquisition time. These specifications resulted in a good compromise between measurement quality and duration of each test run with most rejected data points located in the peripheral sub-channels. The 2σ uncertainty estimate for the local axial velocity measurement was ± 1.5%.

Consistency checks made over the whole test series by considering dimensionless local velocities to remove the (low) boundary conditions variations indicated that:

(i) The test repeatability was good, with most differences in velocity measurements less than 2.5% between repeat tests;

(ii) The measurement redundancy over the nine central measurement points per sub-channel was fairly good. Most related measurements made successively along the *x* and *y* directions agreed within ± 5% over typical inner sub-channels or far downstream from the grids. This scatter, not consistent within the ± 1.5% measurement uncertainty estimate, was attributed to experimental positioning errors mentioned before.

2.3. NESTOR-OMEGA Thermal Experiments

For the thermal experiments in the OMEGA facility, the NESTOR bundles were composed of electrically-heated Inconel 600 tubs, with a 7.7 mm and 8.15 mm inner diameter for the 9 inner rods and the 16 peripheral rods, respectively, resulting in an inner-to-peripheral rod power peaking factor of ~ 1.3. Measurement of the electrical resistance of these heater rods (both Inconel 600 length and copper connectors) allowed an accurate determination of heat flux distribution in the test section.

For both bundle configurations, several steady-state test series were completed in high pressure and temperature water flows covering normal PWR operation conditions, but only that in single-phase flow was considered in the present CFD RR benchmark exercise. The operating conditions of these single-phase test runs were 15.5 MPa in gauge outlet pressure, 900 kW/m^2 in outer-surface heat flux density over the nine inner heater rods (except one test run at 600 kW/m^2), and a cross-sectional-averaged mass velocity ranging from 3,000 to 4,500 kg/m^2/s. The inlet temperature was varied so that the average Reynolds numbers Re_{Sc} over the instrumented area roughly ranged from 300,000 to 600,000.

For each related test run:

- A detailed 2-D temperature distribution over the inner-surface of the heater rod wall was collected over the four uppermost grid spans 1a to 2b for the nine inner rods, by sliding and rotating type N thermocouple (TC) probes inside the rods, in axial and circumferential increments of 25 to 35 mm and 15 to 25°, respectively. The TC probe is shown schematically in Figure 4. The uncertainty in axial and circumferential TC tip location was 1 mm and 1°, respectively.
  A rounded silver disk was brazed at the tip of the 0.89 mm outside diameter (OD) insulated TC sheath to provide a good thermal point contact with the rod inner-surface. However, the actual contact sensing area increased due to a wear during the probe operation, thus resulting in up to ~ 15° circumferential contact angle.
- A fluid temperature map over the bundle cross-section was obtained at the End Of Heating Length (EOHL) of the bundle by point measurement at the center of each sub-channels. The 1 mm OD TCs used were positioned within guiding holes drilled in a specific support grid located 35 mm downstream from the EOHL. As compared to the design locations, the 2σ positioning error in transverse location of the EOHL TC tip was estimated at ± 1.5 mm.

Successive *in-situ* TC calibration test series resulted in a 2σ uncertainty in both EOHL and rod wall surface temperature measurements of ± 0.5 K after including requisite correction for the calibration errors.

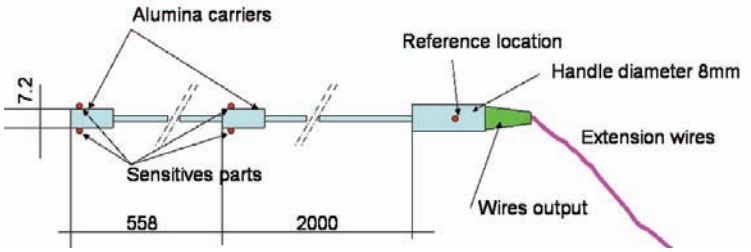

Figure 4. Schematic of the sliding/rotating probe.

These rod inner-surface and EOHL temperatures were acquired and time-averaged over a long enough acquisition time and after a prescribed waiting time, along with the corresponding (steady-state) test operating conditions measured at the test section boundaries - inlet temperature, outlet pressure, mass flow rate, and total bundle heating power. The measurement uncertainties in these test operating conditions were ± 0.2 K, ± 100 kPa, ± 1%, and ± 0.1%, respectively. A filtering process was applied to the raw data to eliminate results obtained during unstable conditions or provided by TCs having a questionable behavior.

The consistency checks performed on the single-phase test data showed that:

(i) The heat balances were very good;
(ii) The redundancy in local rod wall inner-surface temperature measurements at the same location was good;
(iii) There were fairly significant repeatability deviations (which increased with time) in both the EOHL and rod wall inner-surface temperature measurements (SSG bundle), and in the latter measurements only for the MVG bundle. As a result, a special care was taken in selecting test runs most suitable for the CFD RR benchmark exercise;
(iv) Circumferential variations in heater rod wall thickness of a sinusoidal form, likely due to an eccentric inside diameter with respect to the outside diameter of the heater rod existed, as confirmed by dedicated boiling tests and limited post-mortem ultra-sonic measurements. An analytical method using the boiling test rod wall inner-surface temperature distribution was developed to determine the

sinusoidal deviations in rod wall thickness with respect to the 0.9 mm uniform design thickness for each of the 9 inner rods. This consistency check demonstrated that the wall thickness deviations were lower than 0.02 mm.

3. ROUND ROBIN CFD BENCHMARK

3.1. Structure of Round Robin Problems

The RR CFD benchmark exercise against the NESTOR experimental data consists of two Phases depending on the NESTOR bundle grid configuration - simple support grids (Phase 1) and mixing vane grids (Phase 2), as shown in Figure 5. Each phase consisted of two exercises: an isothermal validation based on MANIVEL tests (Exercise 1) and a thermal validation based on OMEGA tests (Exercise 2).

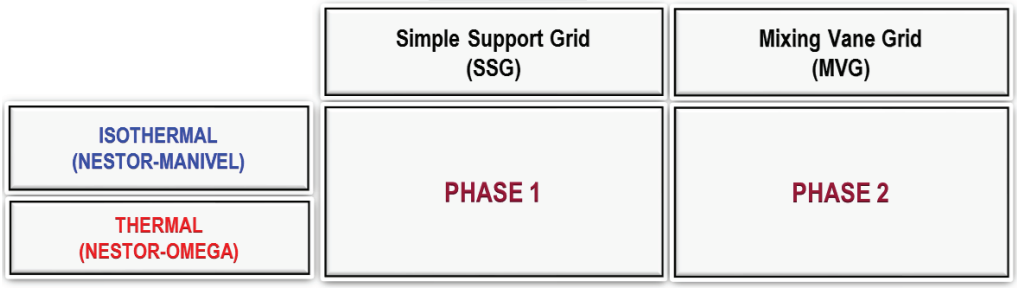

Figure 5. Structure of the EPRI CFD benchmark exercise.

In both Phase 1 and Phase 2, the RR considered four problems: one problem for the MANIVEL isothermal case and three problems for the OMEGA heated case with different thermal hydraulic boundary conditions with respect to mass velocity, heat flux density and inlet temperature. In Phase 1, the isothermal case and the first heated problem were completed within an open data framework, and the two latter heated problems within a blind data framework [7]. In contrast in Phase 2, the RR considered the isothermal problem and the first heated problem under a partially blind data framework, meaning that CFD modeling was initially performed under the blind data framework, but once the calculation results were submitted to the organizer, the experimental data for the two problems were released to the RR Participants. The other two heated problems were performed only under the blind data framework for the entire procedure, as with Phase 1 [8].

3.2. Participants and CFD Codes Used

Ten organizations (ANSYS, AREVA, CD-adapco, CEA, EDF, ENUSA, KEPCO NF, Penn State University, Texas A&M University, and Westinghouse) participated in the Phase 1 benchmark exercise, while seven organizations (ANSYS, AREVA, CD-adapco, EDF, Penn State University, Texas A&M University, and Westinghouse) participated in the Phase 2 benchmark exercise. Three commercial CFD codes (ANSYS CFX[3], ANSYS Fluent, and STAR-CCM+), one open-source CFD code (*Code_Saturne*), and one in-house CFD code (Trio_U[3]) were used as CFD solvers by the Participants.

4. SIGNIFICANT OBSERVATIONS

Rather than highlight any one specific result from the RR, in the highlights below only the important criteria that were identified in the process of evaluating RR results are discussed. The important criteria form the basis for the industry *Best Practices* document which is under development.

[3] Note ANSYS CFX and Trio_U were only used in the Phase 1 work.

4.1. Computational Domain and Associated Boundary Conditions

During the CFD RR benchmark exercise, CFD analyses were predominantly carried out over the whole 5x5 full length *NESTOR* rod bundles [7, 8]. Modeling of the entire 5x5 lateral domain was found to be very important for providing realistic conditions over the lateral boundaries formed by the inner surfaces of the bundle casing, while the axial domain could be limited to a few grid spans for isothermal cases. The actual axial experimental configuration was required for the thermal problems.

Unfortunately attempting to extend these methods to CFD analysis over the entire axial and lateral domain of a PWR core, or even over a single fuel assembly, becomes too extensive and time consuming, despite the currently available computer speed and data storage capacity. Therefore, a suitably representative computational domain can be restricted to the area of interest, such as (i) the top half of the fuel assembly, where the temperatures and heat fluxes are more limiting, and (ii) guide tube centered and/or assembly-to-assembly gap centered regions at and near the core center in the lateral direction. The definition of the boundary conditions for such in-core computational domains can be aided by a porous media modeling approach.

Regardless of the problem specifics it should be noted that ultimately the selection of computational domain must concomitantly account for the difficulties in specifying relevant boundary conditions for the region of interest. The following boundary conditions are highlighted as having a significant impact on the results of the analysis:

(i) Uniform temperature and axial velocity based on the operating conditions, over the domain inlet section when it corresponds to the bottom of the fuel assembly, as well as associated turbulent model variables over this inlet section. Note that in this case, the latter variables have a negligible impact on the far downstream region of interest.

If the computational domain inlet section is defined at a different axial position along the fuel assembly, temperature and velocity boundary conditions cannot be directly obtained at such location. The lateral boundaries conditions cannot be specified regardless of inlet section location. These difficulties can be partially overcome by the utilization of sub-channel type core code results to initialize CFD analysis.

However, such sub-channel analyses provide cross-sectional-averaged mean values over sub-channel cross-sectional and lateral cell faces, and not their turbulent component. Furthermore, these values are highly dependent on the sub-channel type code used, and are therefore susceptible to any inaccuracy inherent to the sub-channel code. This is *a priori* a less crucial concern for the inlet section boundary conditions than for the lateral boundary conditions considering the very likely limited lateral extent of the computational domain for PWR core CFD applications.

(ii) Constant pressure or free-stream conditions over the outlet section;

(iii) A no-slip condition on the fuel rods and grid surfaces;

(iv) An adiabatic condition on the grid surface (see Section 4.2);

(v) An axial distribution of the volumetric heat generation within the fuel pellet or the circumferentially uniform heat flux over the fuel cladding inner surface, to correctly manage the fuel rod-to-fluid heat transfer over the fuel cladding outer surface (see Section 4.2). The related values are based on the axial and transverse power distributions over the core.

4.2. Fuel Rod-to-Fluid Heat Transfer

Accurate prediction of the fuel cladding outer-surface temperature is important to evaluate occurrence and

location of local SNB and hot spots, and eventually estimate of the steaming rate. Applying a heat flux boundary condition on the cladding surface to predict this temperature forces the heat flux to be constant around the rod outer-surface circumference regardless of the circumferential distribution of local fluid flow conditions. In general, however, these circumferential distributions and derived heat transfer coefficient are non-uniform in a fuel assembly.

Since such local non-uniformities could create a significant bias in outer-surface temperature prediction, it is necessary to use conjugate heat transfer (CHT) process, i.e. to jointly (i) solve the heat conduction equation within the solid region, and (ii) CFD-simulate the T/H flow field in the fluid region. For a given elevation, the solid region can be the cladding volume with a uniform circumferential heat flux distribution on its inner surface, or extended to the whole fuel rod volume with provision of a constant volumetric heat source term in the fuel pellet.

The use of CHT insures a more representative circumferential distribution of the heat flux and resulting temperature over the cladding surface. While this has a negligible effect on the heat transfer coefficient variation around the rod (driven by the flow field), heat generated in the fuel pellet is redistributed around the fuel rod cladding circumference, with areas of high heat transfer coefficients removing more heat and vice versa. As a result, while the use of the CHT process does not qualitatively change the circumferential distribution of cladding outer-surface temperature distribution compared to the uniform heat flux boundary condition, it lowers the temperature variation around the rod, as observed during the CFD RR benchmark exercise. Ref [9] discusses additional details of the impact of using the rod conduction in calculating fuel rod outer-surface temperatures.

The accuracy of fuel rod surface temperature predictions when utilizing CHT processes was demonstrated in the CFD RR benchmark exercise [7, 8]. It allows for more realistic prediction of circumferential distributions of fuel rod outer-surface temperatures. CHT could also be used for the grid structure heat transfer, but this effect is negligible, especially in the region of interest far downstream of the grid.

4.3. Turbulence Model Selection and Associated Near-Wall Treatments

Modelling of the turbulence all along the fuel rod bundle domain is crucial, especially as it develops in the wake of the grids. The selected turbulence model must account for the mixing phenomena in the flow field and simulate the local flow field in the near-rod and -grid regions. These are key requirements, which also entail the use of appropriate meshes, and govern the prediction of the friction pressure losses along the rods and across the grids, as well as the cladding outer-surface temperature.

The complex geometry of a PWR fuel assembly with split-type MVGs is subjected to both secondary and lateral flows. The secondary flows of the Prandtl's second kind are generated in rod bundles with rod array pitch-to-rod diameter ratios similar to those of PWR fuel assemblies due to anisotropy of the Reynolds stresses. Despite their small magnitude compared to the bulk flow, these turbulence-driven secondary flows are key phenomena that need to be simulated with an anisotropic turbulence model in "bare" bundle portions. This was proven in Phase 1 of the CFD RR benchmark exercise devoted to the *NESTOR SSG bundle configuration* [7].

The lateral flows are driven by the grid vanes and the subsequent swirling flows across the rod bundle. An isotropic RANS turbulence model, such as the standard k-ε model, is able to capture this phenomenon in CFD simulations, as long as it is used with appropriate wall-region treatments and mesh. This was demonstrated in Phase 2 of the CFD RR benchmark exercise devoted to the *NESTOR MVG bundle configuration* with alternating MVGs and SSGs [8].

The Phase 2 exercise also showed that the isotropic turbulence models and the anisotropic quadratic k-ε models both provided reasonably similar results, when compared to experimental data for both MVG and SSG grid span pressure losses, and mean axial velocity in the wake of the alternating MVGs and SSGs, in the *NESTOR MVG bundle configuration*. The foregoing statement could not be made for the rod wall inner-surface temperatures since all the calculations with CHT were performed using anisotropic turbulence models only. However note that in Phase 1 (*SSG bundle configuration*), the anisotropic turbulence model calculations resulted in significantly better agreements with the measurements than the isotropic turbulence model calculations for the flow field characteristics, and in slightly better agreements only for the rod wall inner-surface temperature, in the far wake of the SSGs [7].

Reynolds stress models are also expected to provide good results in configurations with swirl flows, but the few related simulations involved in the CFD RR benchmark exercise did not confirm this expectation in the *MVG bundle configuration*. Furthermore, it is worth noting these simulations often demanded a significant increase in computing time due to the additional equations and reduced convergence behavior.

The use of wall function along with anisotropic turbulence models was successful in predicting the rod wall inner-surface temperature distribution and axial velocity field in the CFD RR benchmark exercise, but the use of improved near-wall treatments (combining wall function with low-Reynolds number formulation depending on the near-wall mesh size) was not fully tested in this benchmark.

4.4. Mesh Generation

Generation of an appropriate mesh is another key factor affecting the accuracy of the CFD results. The meshing must meet the requirements of the selected turbulence model and near-wall treatments. Also, it has to account for two main characteristics of the industrial applications, namely, complex geometries for the mixing vane grids and the need for large computational domains, both requiring extensive high resolution mesh. Furthermore, the mesh resolution and quality affect the computational stability and convergence time. Eventually, the CFD analyst has to select a mesh type supported by the CFD solver used. But available central processing unit (CPU) resources may currently limit these meshing requirements.

The solid and fluid models are considered separately in the following sub-sections.

4.4.1. Solid Model

The mesh generation of the grid region is a main concern because of the structural complexity. An appropriate solid model, accounting for reasonable simplifications compared to manufacturing computer-aided design (CAD) renderings, has to be defined first. Indeed, modelling all the exact details of the grid designs and grid-to-rod interfaces could be detrimental to subsequent meshing in terms of the quality of the mesh elements. This would result in much larger than necessary fluid model meshing, and unnecessary demands on CPU time or modeling domain size. These in turn would affect the accuracy of the CFD calculation, or even the ability to model the design in CFD.

Experience has shown that appropriate assumptions and simplifications to the solid model of the grid design can greatly reduce mesh size required in each grid cell without affecting the accuracy of the calculation [10]. Typically, grid features that are designed to affect the flow (like mixing vanes) or that form flow blockages (straps, dimples, springs, weld nuggets) in the axial flow need to be modeled, whereas features of the grid design that are not directly in the axial flow path can be ignored. The following specific assumptions and simplifications related to the solid mesh model were found to be important:

(i) Weld nuggets - Instead of their complex shape, adoption of a conic shape allowing much easier meshing, with the appropriate flow blockage;
(ii) Spring/dimple to rod contact – Addition of blocks to the springs and dimples to form a wider contact with the rods than with the theoretical vertical line contact. This makes the mesh in these regions easier and improves its quality;
(iii) Vertical slots in the grid straps - Fill/close the very small gaps (and in particular those at the strap intersections)

As previously indicated, the use of CHT does not have significant impact on the grid-to-rod and grid-to-fluid heat transfer, so grids do not need to be (and were not in the present CFD RR) meshed. On the other hand, to deal with the required fuel rod-to-fluid conjugated heat transfer, the fuel rod-related solid model had to be considered; its definition did not need any simplification except its limitation to the rod wall volume in case a uniform heat flux boundary condition was actually adopted on its inner surface. Its mesh generation was of a different nature, but special attention was given to (i) ensure a sufficient resolution with element thickness similar to that in-fluid close to the wall in the radial direction (it was found that ~5 layers in the 0.9 mm thick wall produced a good representation [7, 8]), and (ii) conform to the fluid model mesh around the fuel rod-to-fluid interface.

4.4.2. Fluid Model

While several mesh types for the fluid model were adopted during the CFD RR benchmark exercise, a dedicated sensitivity analysis was not performed. However, some insights were drawn from the CFD calculations on the MVG bundle configuration:

(i) Trimmed hexahedral meshes with extrusion layers consistently showed better results than other types of mesh once their resolution and quality were reasonable and they conformed to the requirements of the selected turbulence model and near-wall treatment;
(ii) Fully conformal hexahedral meshes, which are also very time-consuming to generate, consistently showed large under-prediction of the pressure losses and turbulence quantities.

Based on the insights above, trimmed hexahedral meshes are preferable for CFD simulations of PWR assembly bundles. The use of trimmed meshes with local refinements in the grid region in particular, elongated cells along the bare rod portions far from the upstream grids, and extrusion layers for crucial heat transfer modeling over the fuel rods was found to be satisfactory in Phase 2. These selections yield a good compromise between mesh resolution and computational expense.

Whatever the type of mesh adopted, the following were found to be important:

(i) Obtain sufficient overall resolutions for boundary layers, and $y+$ insensitive wall treatments;
(ii) Avoid the use of interfaces (where possible) connecting different axial sections along the fuel bundle. If used, they should be conformal to the fullest extent practical;
(iii) Assess the mesh quality before performing a large and complex CFD analysis, and demonstrate that the final results of the calculations are independent of the mesh that is used.

5. CONCLUSIONS

The CFD RR exercise involved participants from fuel suppliers, CFD software developers, universities, research organizations, and utilities. They used different CFD codes and applied their own methodologies, under some general procedural guidance. As a result, the current status of applying CFD analyses to a PWR-type rod bundle has been elucidated. The goal was to provide (i) a good understanding of items most important in such CFD analyses, and (ii) associated *Best Practices* recommendations, for specific

purposes of predicting pressure losses and local fuel rod outer-surface temperatures in PWR fuel assemblies under single-phase convective heat transfer. This scope allowed a clear identification and understanding of the key phenomena, establishing a list of paramount parameters, and providing guidance on crucial methodological factors in performing the stated CFD calculations. These areas included the (i) computational domain and associated boundary conditions, (ii) fuel rod-to-flow heat transfer process, (iii) turbulence model and near-wall treatments, and (iv) mesh.

In developing *Best Practices* recommendations, the lessons learnt from the present RR exercise are being discussed. Even after identifying the crucial parameters for modeling PWR fuel, the CFD analyst will still need certain flexibility to fit the computation to the problem being analyzed. To additionally optimize and/or check the relevance and acceptability of a CFD methodology, it is felt that application by a CFD user should include comparison of pressure drop results for the specific assembly and grid design in question (for which data may be available from the fuel vendor) and solving one standard benchmark problem with comparison to experimental data by meeting evaluation criteria stipulated *a priori*. As EPRI looks to develop its *Best Practices* recommendations, definition of such a problem and associated evaluation criteria is underway. It is worth noting that meeting these evaluation criteria will not likely be a necessary condition to 'accept' a CFD methodology and its analysis results, but will be intended to provide utility personnel less familiar with CFD a certain level of additional confidence in the analysis results performed on their behalf. It will ultimately be up to the utility or fuel vendor to determine if the results are acceptable.

The current state of the art understanding of the multi-physics of a PWR core, especially of fuel crud generation and deposition that lead to CILC failures, is lacking. Thus rigorous derivation of the evaluation criteria from first principles is not possible and therefore the evaluation criteria will necessarily be based on the CFD RR benchmark exercise results with some added conservatism.

ACKNOWLEDGMENTS

This paper describes research sponsored by the EPRI Fuel Reliability Program, PWR Fuel Cladding Corrosion and Crud Technical Advisory Committee. The authors would like to acknowledge significant support from the Round Robin Participants and in particular Shin Kyu Kang from Texas A&M University, without whose support the CFD RR project would not have been possible.

REFERENCES

1. "Fuel Reliability Guideline: PWR Fuel Cladding Corrosion and Crud, Revision 1, Volume 1, Guidance", EPRI, Palo Alto, CA: 2014. 3002002795.
2. "Assessment of Experimental Data to Support Computational Fluid Dynamics Analysis of PWR Rod Bundle Heat Transfer Studies", EPRI, Palo Alto, CA: 2010. 1021040.
3. A. Bergeron et al, "Design, Feasibility and Testing of Instrumented Rod Bundles to Improve Heat Transfer Knowledge in PWR Fuel Assemblies", *Proceedings of the International LWR Fuel Performance Meeting*, San Francisco, California (2007).
4. P. Peturaud et al, "Analysis of Single-Phase Heat Transfer and Onset of Nucleate Boiling in Rod Bundles*", Proceedings of the 14th International Conference on Nuclear Engineering*, Xi'an (2010).
5. P. Péturaud, "Analyses of Single-Phase Heat Transfer and Onset of Nucleate Boiling in a Rod Bundle with Mixing Vane Grids", *Proceedings of the 14th International Topical Meeting on Nuclear Reactor Thermal Hydraulics*, Toronto (2011).
6. G. Cubizolles et al, "Reproducibility of heat transfer tests in a 5x5 bundle geometry", *Proceedings of the 14th International Topical Meeting on Nuclear Reactor Thermal Hydraulics*, Toronto (2011).
7. "Computational Fluid Dynamics Benchmark of High Fidelity Rod Bundle Experiments: Industry round Robin Phase 1 – Rod Bundle with Simple Support Grids", EPRI, Palo Alto, CA: 2014. 3002000504.
8. "Computational Fluid Dynamics Benchmark of High Fidelity Rod Bundle Experiments: Industry round Robin Phase 2 – Rod Bundle with Mixing Vane Grids", EPRI, Palo Alto, CA: 2015. 3002005401.
9. Conner, M.E., Smith, III, L.D., Young, M.Y., "Azimuthal Heat Transfer Variation Downstream of Grids with Mixing Vanes", *Proceedings of the 2004 International Meeting on LWR Fuel Performance*, Orlando, Florida, USA, September 19-22, 2004.
10. M. E. Conner, Z. E. Karoutas, and Y. Xu, "Westinghouse CFD Modeling and Results for EPRI NESTOR CFD Round Robin Exercise of PWR Rod Bundle Testing", *16th International Topical Meeting on Nuclear Reactor Thermal Hydraulics (NURETH-16)*, Chicago, Illinois, USA, August 30 – September 4, 2015. Paper 13601.